

# Doxorubicin-loaded aromatic imine-contained amphiphilic branched star polymer micelles: synthesis, self-assembly, and drug delivery

Liang Qiu  
Chun-Yan Hong  
Cai-Yuan Pan

Chinese Academy of Sciences Key  
Laboratory of Soft Matter Chemistry,  
Department of Polymer Science and  
Engineering, University of Science and  
Technology of China, Hefei, Anhui,  
People's Republic of China

**Abstract:** Redox- and pH-sensitive branched star polymers (BSPs), BP(DMAEMA-co-MAEBA-co-DTDMA)(PMAIGP)<sub>n</sub>s, have been successively prepared by two steps of reversible addition-fragmentation chain transfer (RAFT) polymerization. The first step is RAFT polymerization of 2-(N,N-dimethylaminoethyl)methacrylate (DMAEMA) and p-(methacryloxyethoxy) benzaldehyde (MAEBA) in the presence of divinyl monomer, 2,2'-dithiodiethoxyl dimethacrylate (DTDMA). The resultant branched polymers were used as a macro-RAFT agent in the subsequent RAFT polymerization. After hydrolysis of the BSPs to form BP(DMAEMA-co-MAEBA-co-DTDMA)(PMAGP)<sub>n</sub>s (BSP-H), the anticancer drug doxorubicin (DOX) was covalently linked to branched polymer chains by reaction of primary amine of DOX and aldehyde groups in the polymer chains. Their compositions, structures, molecular weights, and molecular weight distributions were respectively characterized by nuclear magnetic resonance spectra and gel permeation chromatography measurements. The DOX-loaded micelles were fabricated by self-assembly of DOX-containing BSPs in water, which were characterized by transmission electron microscopy and dynamic light scattering. Aromatic imine linkage is stable in neutral water, but is acid-labile; controlled release of DOX from the BSP-H-DOX micelles was realized at pH values of 5 and 6, and at higher acidic solution, fast release of DOX was observed. In vitro cytotoxicity experiment results revealed low cytotoxicity of the BSPs and release of DOX from micelles in HepG2 and HeLa cells. Confocal laser fluorescence microscopy observations showed that DOX-loaded micelles have specific interaction with HepG2 cells. Thus, this type of BSP micelle is an efficient drug delivery system.

**Keywords:** RAFT polymerization, controlled release, doxorubicin, branched star polymer, pH-sensitive

## Introduction

In the past decades, various drug delivery approaches have been developed to achieve target delivery, highly therapeutic efficacy, and minimal side effects.<sup>1</sup> As one of the most promising nanocarrier systems, self-assembled polymeric micelles have attracted significant attention due to their unique features, such as enhancing aqueous solubility of the drug, prolonging circulation time, reducing systemic adverse effects, and preferential accumulation at the tumor site owing to the enhanced permeability and retention effect.<sup>2-6</sup> Various architectural polymers including linear polymers, dendrimers, hyperbranched polymers, and dendronized polymers have been utilized to construct nanocarriers.<sup>7-11</sup> Compared to the linear polymers, branched polymers possess some advantages, including a number of surface groups and hollow voids of the branching architecture, which make them attractive in drug delivery applications.<sup>12-16</sup>

Correspondence: Cai-Yuan Pan;  
Chun-Yan Hong  
Chinese Academy of Sciences Key  
Laboratory of Soft Matter Chemistry,  
Department of Polymer Science and  
Engineering, University of Science and  
Technology of China, Hefei Anhui  
230026, People's Republic of China  
Tel +86 551 6360 3264;  
+86 551 6360 6081  
Email pcy@ustc.edu.cn;  
hongcy@ustc.edu.cn

Generally, there are two strategies to prepare the hydrophobic drug-loaded polymeric micelles; one strategy is encapsulation of the drug within the hydrophobic cores of micelles or nanoparticles,<sup>17–19</sup> and the resultant products can improve the water-solubility and enhance the stability of drug.<sup>20</sup> The other strategy is to link the drug onto the hydrophobic core of micelles via a labile linkage that can be cleaved in the presence of external stimuli, such as redox state of the media, light, and specific molecules, and then the drug is released under environmental stimuli.<sup>21–24</sup> For example, controlled release of the drug from nanostructural materials was achieved via the breaking of a photo-cleavable linker, 2-nitrobenzyl ester, under irradiation of 365 nm light,<sup>21</sup> or via the breaking of reducible disulfylbutyrate linker in the presence of glutathione.<sup>22</sup> Among the stimuli-responsive nanostructural materials, the pH-sensitive polymeric assemblies have attracted extensive interest because of their particular relevance in biological applications and the significantly lower pH of the tumor cells as compared to normal cells.<sup>25,26</sup> The acid-labile linkages utilized to chemically conjugate drugs onto the polymers or assemblies include hydrazones,<sup>27–29</sup> acetal,<sup>30,31</sup> ketal,<sup>32</sup> and imines.<sup>33</sup> Although the acidic hydrolysis of imines is well known in organic chemistry, this imine linker is rarely utilized to conjugate drugs onto polymeric assemblies, because this linker has been reported to cleave at physiological pH.<sup>34,35</sup>

In recent years, the imine linkers have gained significant attention, because several studies indicate that the aromatic imines with extended  $\pi$ - $\pi$  conjugation can significantly improve the stability of imine linkages in water.<sup>36–39</sup> Therefore, we speculated that investigation of pH-responsive behaviors of drug carriers, in which the drug is covalently attached to the polymer backbone in the hydrophobic cores via aromatic imine linkage, should be interesting, and would help to enable design of a pH-triggered drug delivery system. The imine linkage has been widely employed in the preparation of shell or core cross-linked (SCL or CCL) micelles for improvement of micellar integrity and drug encapsulation stability. Encapsulation of a drug in CCL or SCL micelles was conducted through the reaction of primary amines in the polymers with a dialdehyde cross-linker.<sup>40,41</sup> CCL and SCL micelles are also prepared by the reaction between linear polymers carrying the primary amine and aldehyde group, respectively.<sup>42,43</sup> However, no report in the literature we consulted studies synthesis of polymeric micelles containing reactive aldehyde groups in core polymers for conjugation of molecules, eg, drug, peptides, or carbohydrates. Thus, a known aldehyde-containing monomer, p-(methacryloxyethoxy)benzaldehyde (MAEBA)

was chosen in order to incorporate reactive aromatic aldehyde groups into polymer chains, and then an anti-cancer drug, doxorubicin (DOX) was covalently attached to the polymer chains by reaction of aldehyde in the polymer chains with the primary amine of DOX.

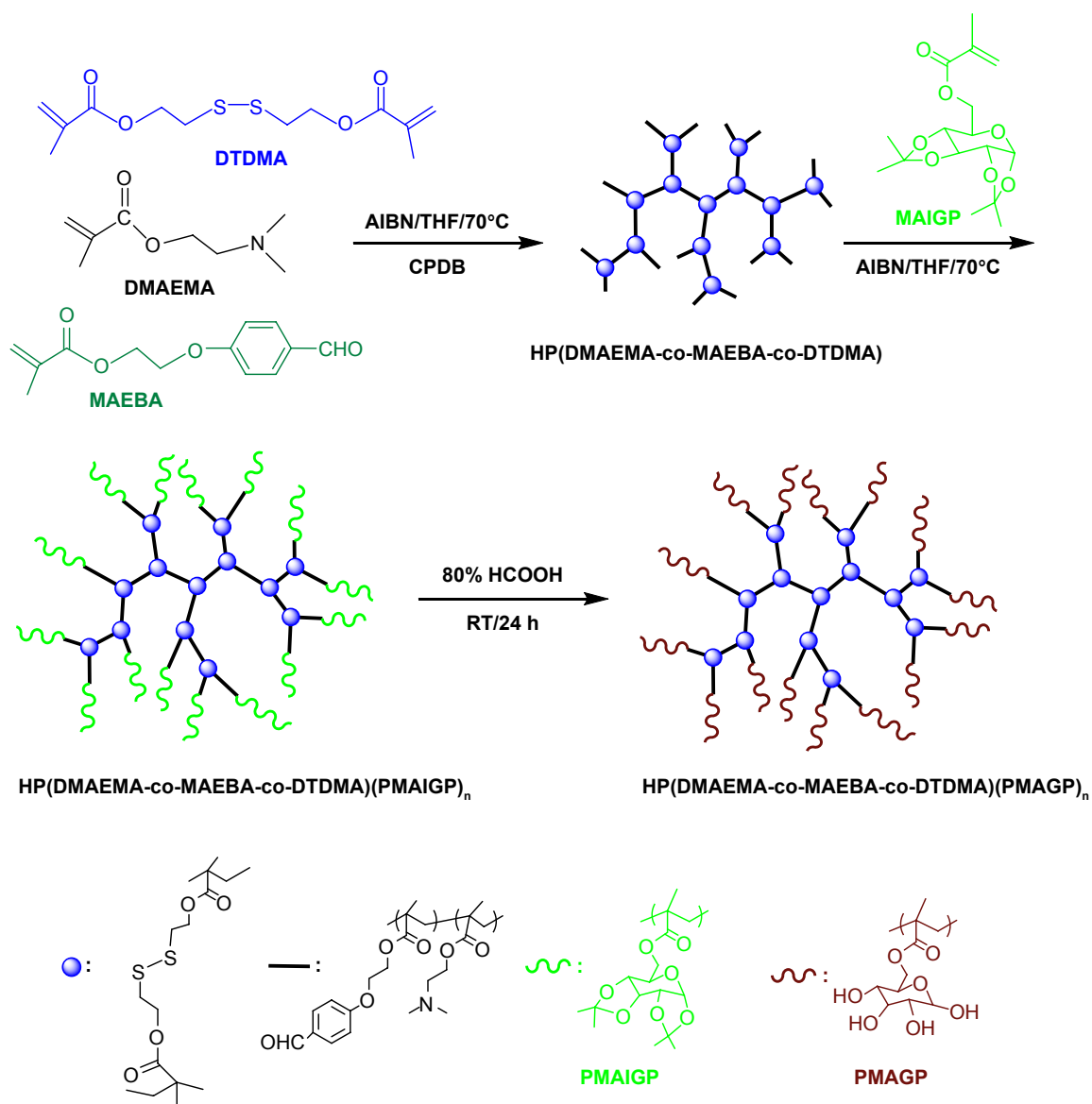
Very few studies on synthesis of copolymers containing MAEBA units have been reported;<sup>44–46</sup> for example, reversible addition–fragmentation chain transfer (RAFT) polymerization of MAEBA and oligo(ethylene glycol) monomethyl ether methacrylate (OEGMA) produced water soluble random copolymers, and their thermo-responsive properties were studied.<sup>44</sup> The block copolymer, poly(caprolactone)-(PCL)-*b*-poly(OEGMA-*co*-MAEBA) was synthesized by atom transfer radical polymerization.<sup>45</sup> All of these polymers used in the studies are linear; no study on branched copolymers containing MAEBA has been reported, to the best of our knowledge.

In the present article, we synthesize pH and redox dual-responsive micelles based on the branched star polymers (BSPs) containing biodegradable disulfide linkages through two steps of RAFT polymerization, as shown in Figure 1. The branched polymers are composed of MAEBA, 2,2'-dithiodiethoxyl dimethacrylate (DTDMA), and 2-(N,N-dimethylaminoethyl)methacrylate (DMAEMA). The disulfide is a well-known reduction-responsive linkage;<sup>24,45</sup> thus, degradation of the DTDMA units can ensure renal clearance of the polymers after drug delivery. The anti-cancer drug DOX was grafted onto the BSP by the reaction of the aldehyde group in MAEBA with the primary amine in DOX to form an acidic-labile imine bond. After self-assembling of the resultant BSPs in water, micelles with a DOX-containing branched polymer as a core and poly(6-O-methacryloyl-D-galactopyranose) (PMAGP) as a shell were formed. Since the galactosylated units of PMAGP in the shell of micelles are selectively recognized by asialoglycoprotein receptor (ASGP-R) on the surfaces of HepG2 cells,<sup>24</sup> the dual-responsive BSP micelles possessed a target delivery property.

## Materials and methods

6-O-Methacryloyl-1,2; 3,4-di-O-isopropylidene-D-galactopyranose (MAIGP) was prepared as previously reported,<sup>24</sup> and its hydrogen-1 NMR (<sup>1</sup>H-NMR) (300 MHz, CDCl<sub>3</sub>,  $\delta$ , ppm) was as follows: 1.21–1.60 (m, 12H,  $-\text{CH}_3$ ); 1.95 (s, 3H,  $-\text{CH}_3$ ); 4.08, 4.19–4.42, 4.63, and 5.54 (7H, sugar moiety); and 5.57 and 6.14 (s, 2H,  $=\text{CH}_2$ ). p-(methacryloxyethoxy)benzaldehyde (MAEBA) was prepared according to the reported procedure,<sup>43</sup> and its <sup>1</sup>H-NMR (300 MHz, CDCl<sub>3</sub>,  $\delta$ , ppm) was as follows: 1.92 (s, 3H,  $-\text{CH}_3$ ); 4.29 (t, 2H,  $-\text{O}-\text{CH}_2$ ); 4.51 (t, 2H,  $-\text{O}-\text{CH}_2$ );

A



B

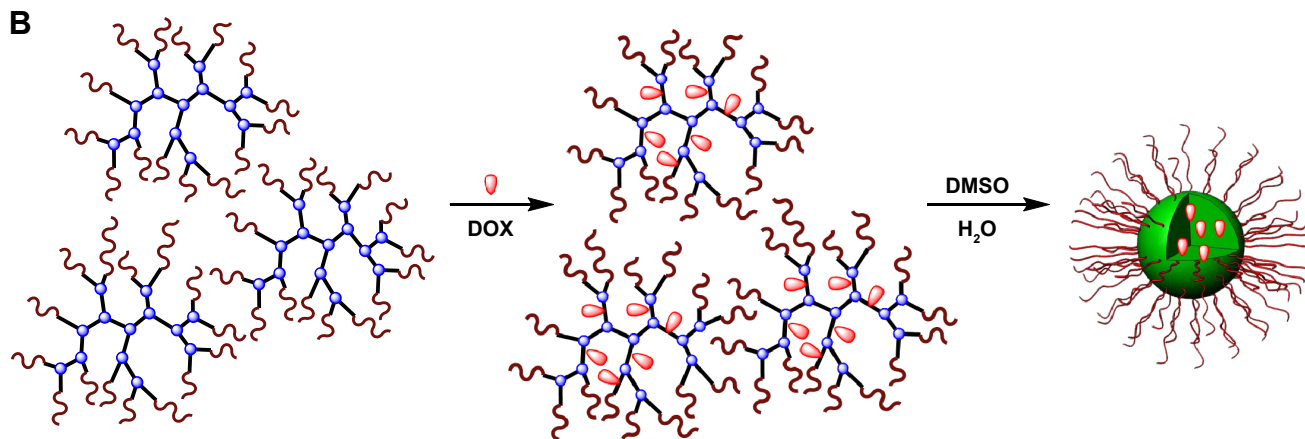


**Figure 1** Synthesis of BP(DMAEMA-co-MAEBA-co-DTDMA)(PMAGP)<sub>n</sub> (A); loading of DOX and formation of DOX-loaded BP(DMAEMA-co-MAEBA-co-DTDMA)(PMAGP)<sub>n</sub> micelles (B).

**Abbreviations:** BP, branched polymer; AIBN, Azobis(isobutyronitrile); BP(DMAEMA-co-MAEBA-co-DTDMA)(PMAGP)<sub>n</sub>, branched poly(2-[N,N-dimethylaminoethyl] methacrylate-co-p-[methacryloxyethoxy]benzaldehyde-co-2,2'-dithiodiethoxyl dimethacrylate)(poly[6-O-Methacryloyl-D-galactopyranose])<sub>n</sub>; THF, tetrahydrofuran; DMAEMA, 2-(N,N-dimethylaminoethyl)methacrylate; MAEBA, p-(methacryloxyethoxy)benzaldehyde; DTDMA, 2,2'-dithiodiethoxyl dimethacrylate; PMAGP, poly(6-O-methacryloyl-D-galactopyranose); CPDB, cyanoisopropyl dithiobenzoate; DOX, doxorubicin; DMSO, dimethyl sulfoxide; h, hours; PMAIGP, poly(6-O-methacryloyl-1,2;3,4-di-O-isopropylidene-D-galactopyranose); MAEBA, p-(methacryloxyethoxy)benzaldehyde; RT, room temperature.

5.57 and 6.12 (s, 2H, =CH<sub>2</sub>); 7.00 and 7.81 (d, 4H, -C<sub>6</sub>H<sub>4</sub>); and 9.86 (s, 1H, -CHO). 2,2'-Dithiodiethoxyl dimethacrylate (DTDMA) was synthesized according to the literature,<sup>13</sup> and its <sup>1</sup>H-NMR (300 MHz, CDCl<sub>3</sub>, δ, ppm) was as follows: 1.88 (s, 6H, -CH<sub>3</sub>); 2.88–2.93 (t, 4H, -S-CH<sub>2</sub>-); 4.31–4.36 (t, 4H, -O-CH<sub>2</sub>-); and 5.52 and 6.07 (s, 4H, =CH<sub>2</sub>). 2-(N,N-Dimethylaminoethyl) methacrylate (DMAEMA, 97%, Alfa) was purified by passing it through a basic alumina column; then, it was vacuum-distilled and was stored at -18°C prior to use. Tetrahydrofuran (THF) was refluxed over sodium for 24 hours and distilled prior to use. Azobis(isobutyronitrile) (AIBN; Sigma-Aldrich Co, St Louis, MO, USA) was recrystallized from ethanol. Cyanoisopropyl dithiobenzoate (CPDB) was prepared according to our previous report.<sup>13</sup> Doxorubicin hydrochloride (DOX·HCl) and 2-(4-amidinophenyl)-6-indolecarbamide dihydrochloride (DAPI) were respectively purchased from Aladdin (Alladin Industrial Corporation, Shanghai, People's Republic of China) and Sigma-Aldrich Co, respectively; both were used as received. All other reagents with analytical grade were purchased from Shanghai Chemical Reagent Co (Shanghai, People's Republic of China) and were used as received.

## Characterization

<sup>1</sup>H-NMR measurements were carried out on a Bruker AV300 NMR spectrometer (Bruker Corporation, Billerica, MA, USA) using CDCl<sub>3</sub> or D<sub>2</sub>O or dimethyl sulfoxide (DMSO)-d<sub>6</sub> as solvent. Molecular weight ( $M_w$ ) and molecular weight distribution ( $M_w/M_n$ ) were determined on a Waters Corporation (Milford, MA, USA) 150C gel permeation chromatography (GPC) instrument equipped with microstyragel columns (500, 10<sup>3</sup>, and 10<sup>4</sup> Å) and an RI 2414 detector set at 30°C; monodispersed polystyrene standards were used in the calibration of the number-average molecular weight ( $M_n$ ),  $M_w$ , and  $M_w/M_n$ , and THF was used as an eluent at a flow rate of 1.0 mL/min. Ultraviolet (UV)/visible (Vis) light measurement was performed on a Unico (United Products & Instruments, Inc., NJ, USA) UV/Vis 2802PCS spectrophotometer. Transmission electron microscopy (TEM) observations were conducted on a JEM-100SX electron microscope at an acceleration voltage of 100 kV. The sample for TEM observation was prepared by placing 10 μL of micellar solution on a copper grid coated with thin films of Formvar and carbon. Dynamic light scattering (DLS) measurements were carried out on a DynaPro light scattering instrument (model DynaPro-99E) at 25°C with an 824.3 nm laser, and the data were analyzed with DYNAMICS V6 software.

## Synthesis of branched polymers BP(DMAEMA-co-MAEBA-co-DTDMA)s

A typical polymerization procedure is as follows. Into a 5 mL polymerization tube, DMAEMA (678 mg, 4.32 mmol), DTDMA (52 mg, 0.18 mmol), MAEBA (113 mg, 0.48 mmol), CPDB (26.5 mg, 0.12 mmol), AIBN (4.9 mg, 0.03 mmol) and THF (2.5 mL) were successively added. The mixture was degassed through three freeze-pump-thaw cycles. The polymerization tube was then flame-sealed under vacuum, and the sealed tube was immersed in an oil bath at 70°C. After 24 hours, the polymerization tube was cooled to room temperature rapidly, and the polymer was obtained by precipitation from n-hexane. The obtained product was dried overnight in a vacuum oven at room temperature.

## Synthesis of BP(DMAEMA-co-MAEBA-co-DTDMA)(PMAIGP)<sub>n</sub>

A typical polymerization procedure was followed. Into a 2 mL polymerization tube, BP(DMAEMA-co-MAEBA-co-DTDMA)-1 (BP-1) ( $M_n$  = 8,000 g/mol, 32 mg, 4 μmol), MAIGP (262 mg, 0.8 mmol), AIBN (0.1336 mg, 0.8 μmol), and THF (2 mL) were added. After three freeze-vacuum-thaw cycles, the polymerization tube was sealed under vacuum. The polymerization was carried out at 70°C for a prescribed time. The polymerization tube was cooled to room temperature rapidly, and then the reaction mixture was precipitated into an excess of n-hexane. The obtained product was dried overnight in a vacuum oven at room temperature.

## Hydrolysis of BP(DMAEMA-co-MAEBA-co-DTDMA)(PMAIGP)<sub>n</sub>

The BP(DMAEMA-co-MAEBA-co-DTDMA)(PMAIGP)<sub>n</sub> (200 mg) was stirred in 80% formic acid (10 mL) for 48 hours at room temperature; then, deionized water (3 mL) was added, and the mixture was stirred for an additional 3 hours. The final solution was dialyzed against deionized water for 3 days to remove the formic acid. The product was obtained as a white cotton-like solid by lyophilization.

## Fabrication of BP(DMAEMA-co-MAEBA-co-DTDMA)(PMAGP)<sub>n</sub> micelles

BP(DMAEMA-co-MAEBA-co-DTDMA)(PMAGP)<sub>n</sub> (20 mg) was dissolved in DMSO (2 mL). Under vigorous stirring, deionized water (8 mL) was slowly added. The dispersion was stirred for another 3 hours; then, DMSO was

removed by dialysis ( $M_w$  cutoff 3,500 Da) against deionized water for 48 hours.

## Preparation of DOX-loaded micelles

BP(DMAEMA-co-MAEBA-co-DTDMA)(PMAGP)<sub>n</sub> (30 mg) was dissolved in 5 mL of DMSO at room temperature, and then DOX·HCl (30 mg) and an equal molar amount of triethylamine were added. The mixture was stirred for 3 hours and subsequently was slowly added into 10 mL of phosphate-buffered saline (PBS; 50 mM, pH 7.4). After having been stirred for another 2 hours, the resultant solution was dialyzed against deionized water for 18 hours ( $M_w$  cutoff 3,500 Da) at room temperature, and the deionized water was changed every 2 hours. The contents inside the dialysis bag were filtered and lyophilized. The amount of DOX was determined by UV/Vis quantitative analysis (excitation at 497 nm), and the standard curve was obtained by plotting the UV absorbance at 497 nm with different concentrations of DOX in DMSO solutions. To determine the total loading of the drug, the DOX-loaded micelles were dissolved in DMSO, and the concentration of DOX in DMSO was determined based on the UV absorbance at 497 nm. Drug loading content (DLC) and grafting efficiency (GE) of DOX were calculated according to Equations 1 and 2, respectively:

$$\text{DLC (wt\%)} = \frac{\text{Weight of loaded drug}}{\text{Weight of polymer}} \times 100\% \quad (1)$$

$$\text{GE (wt\%)} = \frac{\text{Weight of loaded DOX}}{\text{Weight of DOX added}} \times 100\% \quad (2)$$

## Degradation of BP(DMAEMA-co-MAEBA-co-DTDMA)(PMAGP)<sub>n</sub>

BP(DMAEMA-co-MAEBA-co-DTDMA)(PMAGP)<sub>n</sub> (20 mg) was dissolved in 10 mL of the deionized water at room temperature; subsequently, 10 mM dithiothreitol (DTT) was added. The mixture was stirred for 48 hours. After reaction, the product was dealt with using dialysis ( $M_w$  cutoff 3,500 Da) against deionized water for another 48 hours, and then the product was dried by freeze drying.

## In vitro release measurements

The drug release was performed under both reduction-insensitive and reduction-sensitive conditions. For the reduction-sensitive experiment, the drug release was performed under various pH values (pH values of 5, 6, and 7.4). A typical procedure in the current study was as follows: an aqueous dispersion of DOX-loaded micelles (2.0 mg/mL,

3.0 mL) was transferred to a dialysis bag with a  $M_w$  cutoff of 3.5 kDa, and then the dialysis bag was immersed in 60 mL of various buffer solutions (with pH values of 5, 6, and 7.4) containing 10 mM DTT (90 mg), which was purged with pure nitrogen for 30 minutes prior to use. The samples (2 mL) were taken at predetermined time intervals for estimating the amount of drug released, and the same method was employed for the reduction-insensitive experiment, except for the use of pure PBS solution to replace the buffer solution. UV absorbance of the dialysis solution at 497 nm was monitored to determine the DOX releasing profile. A series of parallel experiments was conducted. Each measurement was done in triplicate, and the data are shown as the mean value plus a standard deviation ( $\pm$  SD).

## Cellular uptake

Cellular uptake behaviors of DOX-loaded micelles (BSP-3-DOX) by HepG2 or HeLa cells were examined by confocal laser scanning microscopy (CLSM; Leica TCP SP5 [Leica Microsystems, Wetzlar, Germany]). HepG2 and HeLa cells were cultured in Dulbecco's Modified Eagle's Medium (DMEM) supplemented with 10% fetal bovine serum (FBS) for 24 hours at 37°C under an atmosphere with 5% CO<sub>2</sub> in a 96-well plate, then changed to freshly prepared DMEM which contains 15.9 µg/mL of pure DOX (100 µg/mL of the BSP-3-DOX contains 15.9 µg/mL of the pure DOX), which are respectively equivalent to DOX concentrations of 15.9 µg/mL. After being treated for 4 hours, the culture medium was removed; the cells, after being rinsed two times with PBS, were fixed with formaldehyde, and the cell nuclei were stained with DAPI (4',6-diamidino-2-phenylindole) (blue stain). The cells were rinsed with PBS buffer, and were observed using a CLSM (Leica TCP SP5) at 595 nm (excitation wavelength [ $E_x$ ] = 485 nm).

## In vitro cytotoxicity evaluation

The cell viability of HepG2 cells or HeLa cells incubated with DOX·HCl, BSP-3 micelles and DOX-loaded micelles (BSP-3-DOX) was tested using the standard thiazolyl blue MTT assay. HepG2 cell or HeLa cells were cultured in DMEM supplemented with 10% FBS at 37°C under an atmosphere with 5% CO<sub>2</sub>. The cells were seeded in 96-well plates at a density of 5,000 cells per well for 24 hours before treatment. The cells were treated with various concentrations of DOX·HCl, BSP-3 and BSP-3-DOX for 24 hours in 96-well plates. The culture medium in each well was removed and replaced by 100 µL of DMSO. The plate was gently agitated for 15 minutes, and the absorbance values were recorded at a wavelength of 490 nm using a Thermo Electron MK3

spectrophotometer (Thermo Fisher Scientific, Waltham, MA, USA). Cell viability was calculated as

$$\frac{A_{490,\text{treated}}}{A_{490,\text{control}}} \times 100\%, \quad (3)$$

where  $A_{490,\text{treated}}$  and  $A_{490,\text{control}}$  are the absorbance values with or without the addition of micelles, respectively. Each experiment was done in triplicate. The data are shown as the mean value plus  $\pm$  SD. Cell viability was thereby determined.

## Results and discussion

### Synthesis of BP(DMAEMA-co-MAEBA-co-DTDMA)(PMAGP)<sub>n</sub>

Similar to the synthesis strategy used to produce the dendrimer-star copolymers in our previous reports,<sup>47,48</sup> the first step in the current report was synthesis of the branched copolymers, which were prepared by RAFT copolymerization of DMAEMA, MAEBA, and DTDMA, using CPDB as the RAFT agent, as shown in Figure 1A. The DTDMA is a divinyl monomer and was therefore used as divergent agent. It is well known that controlled radical copolymerization of the divinyl and monovinyl monomers in an appropriate recipe produces branched copolymers, and degree of branching (DB) is determined by the ratio of divinyl monomer/monovinyl monomer.<sup>49,50</sup> The feed molar ratio of [DMAEMA+MAEBA]/[CPDB]/[DTDMA] was fixed at 40/1/1.5, but the feed molar ratio of [DMAEMA]/[MAEBA] was varied for achieving various contents of the aldehyde groups, and the detailed polymerization conditions and results are listed in Table 1. Similar to the branched copolymerization with divinyl monomer as a divergent agent in a previous report,<sup>49</sup> high yields (~99%) of the resultant branched copolymers were obtained (Table 1). Their  $M_w$  and  $M_w/M_n$  were characterized by GPC, all the GPC traces in Figure S1 display bimodally, and their  $M_w/M_n$  are broad, which is consistent with controlled radical copolymerization of the mono- and divinyl monomers,

because the branched polymers are formed via step polymerization of the linear polymer chains.<sup>49,50</sup>

To understand branched structure and compositions of the obtained polymers, their <sup>1</sup>H-NMR spectra were measured, and a typical <sup>1</sup>H-NMR spectrum of the branched copolymer, BP-3, is shown in Figure 2A. The DMAEMA, MAEBA, and DTDMA units in the branched copolymer are supported by their characteristic proton signals: the proton signals of the aldehyde and aromatic groups in the MAEBA units are at  $\delta$  =9.86 (a),  $\delta$  =7.82 (b), and  $\delta$  =6.99 ppm (c); the proton signals of methyl and methylene are next to nitrogen, as well as ester methylene in DMAEMA units at  $\delta$  =2.25 (g),  $\delta$  =2.53 (f), and  $\delta$  =4.04 ppm (e); and the proton signals of methylene are next to sulfur and ester methylene in DTDMA units at  $\delta$  =2.5–3.5 (l) and  $\delta$  =4.24 ppm (d), respectively. Compositions of the resultant branched copolymers were calculated based on integral values of the signals at  $\delta$  =9.86 (a),  $\delta$  =2.57 ppm (f), and  $\delta$  =2.5–3.5 ppm (l); the results are listed in Table 1. We can see that the molar ratios of [DMAEMA]:[MAEBA] in the polymers are higher than that in the feed, indicating lower reactivity of MAEBA in comparison with DMAEMA, probably owing to bulky side group of the MAEBA monomer. The <sup>13</sup>C-NMR spectrum of BP-3 also supports the idea that the branched polymers are composed of DMAEMA, MAEBA, and DTDMA units: the characteristic carbon signal of methyl carbon is next to nitrogen in the DMAEMA unit at  $\delta$  =45.5 ppm (m); the characteristic aldehyde carbon signal of the MAEBA unit is at  $\delta$  =190.7 ppm (a); and the carbon signal of methylene is next to sulfur in the DTDMA unit at  $\delta$  =34 ppm.

Since the branching point is formed only when the pendant vinyl groups of the divinyl monomer units in the polymer chains participate in reaction,<sup>49</sup> no vinyl proton signals are observed in the range of 5–6.7 ppm in Figure 2A, indicating that all DTDMA units in the polymer chains become branching units. Therefore, the content of divinyl monomer, in which

**Table 1** Synthetic conditions and results of BP(DMAEMA-co-MAEBA-co-DTDMA)

No	Feed molar ratio of D:B:T:C:AIBN <sup>a</sup>	Yield (%) <sup>b</sup>	$M_n$ (GPC) (g/mol) <sup>c</sup>	$M_w/M_n^c$	DP of primary chain <sup>d</sup>	Molar ratio of [D]:[B]:[T] in polymer <sup>e</sup>
BP-1	36:4:1.5:1:0.25	99	8,000	1.99	37	10:1:0.9
BP-2	32:8:1.5:1:0.25	99	7,600	2.04	43	5:1:0.49
BP-3	16:24:1.5:1:0.25	99	13,100	1.98	36	0.8:1:0.15

**Notes:** <sup>a</sup>D, B, T, and C refer to DMAEMA, MAEBA, DTDMA, and CPDB, respectively. Polymerization temperature was 70°C; time was 24 hours. <sup>b</sup>Determined by gravimetry. <sup>c</sup>Determined by GPC, calibrated based on the narrow polystyrene standards. <sup>d</sup>Calculated according to  $DP = (19.86+12.57/2+12.5-3.5/4)/(17.52/2)$ . <sup>e</sup>Molar ratios of [DMAEMA]:[MAEBA]:[DTDMA] in the polymers were calculated according to <sup>1</sup>H-NMR data.

**Abbreviations:** BP(DMAEMA-co-MAEBA-co-DTDMA), branched poly(2-[N,N-dimethylaminoethyl]methacrylate-co-p-[methacryloxyethoxy]benzaldehyde-co-2,2'-dithiodiethoxyl dimethacrylate); BP, branched polymer;  $M_w/M_n$ , molecular weight distribution; DMAEMA, 2-(N,N-dimethylaminoethyl)methacrylate; MAEBA, p-(methacryloxyethoxy)benzaldehyde; DTDMA, 2,2'-dithiodiethoxyl dimethacrylate; CPDP, cyanoisopropyl dithiobenzoate; GPC, gel permeation chromatography; <sup>1</sup>H-NMR, hydrogen-1 nuclear magnetic resonance; AIBN, Azobis(isobutyronitrile);  $M_w$ , weight-average molecular weight;  $M_n$ , number-average molecular weight; DP, number-average degree of polymerization.

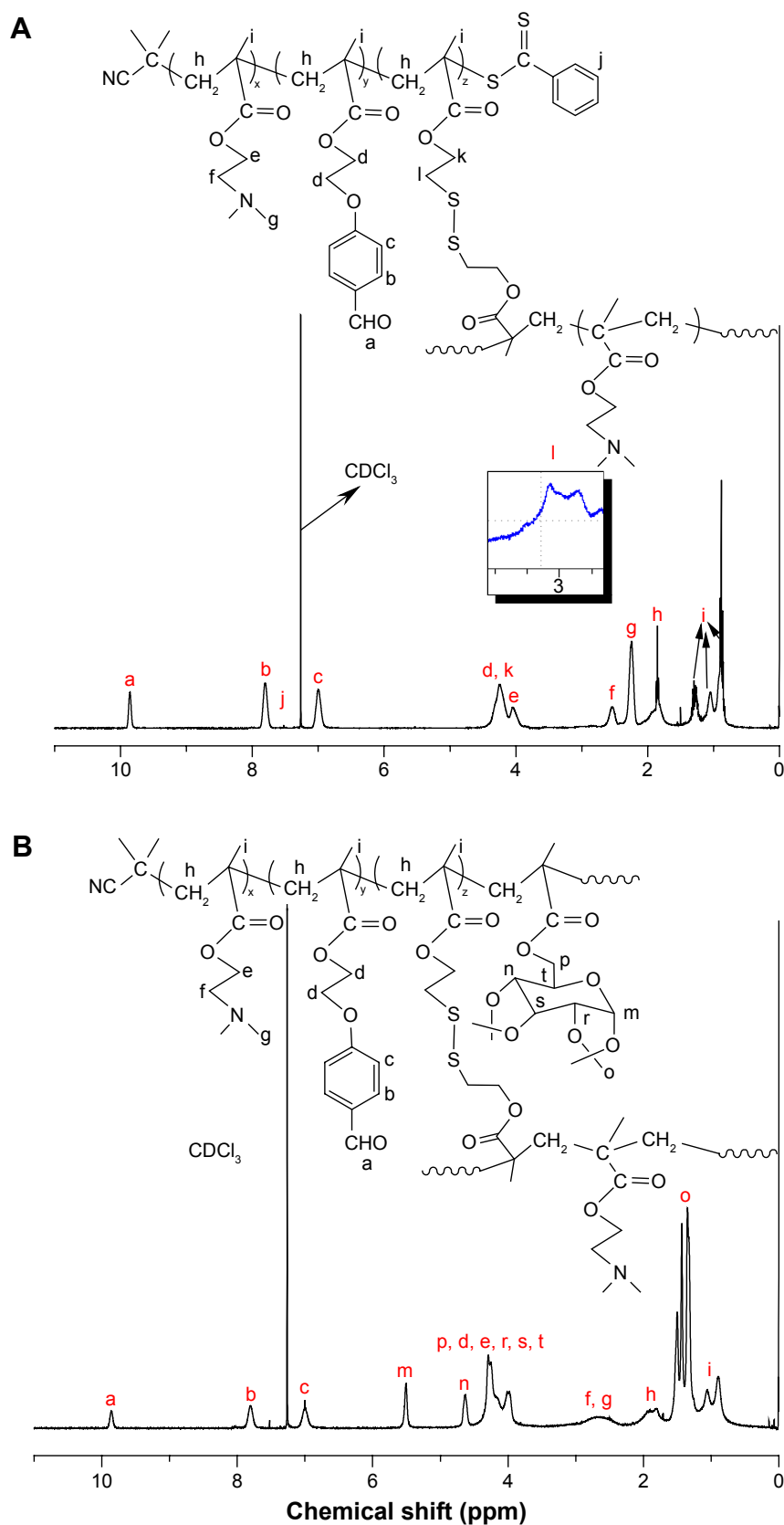


**Figure 2**  $^1\text{H-NMR}$  spectra of the branched polymer, BP(DMAEMA-co-MAEBA-co-DTDMA), BP-3 (**A**), and the branched star polymer, (DMAEMA-co-MAEBA-co-DTDMA) (PMALGP)<sub>3</sub>, BSP-3 (**B**).

**Abbreviations:** PMAIGP, poly(6-O-methacryloylproperty-1,2; 3,4-di-O-isopropylidene-D-galactopyranose);  $^1\text{H-NMR}$ , hydrogen-1 nuclear magnetic resonance; BP, branched polymer; DTDMA, 2,2'-dithiodiethoxy dimethylacrylate; DMAEMA, 2-(N,N-dimethylamino)ethyl methacrylate; MAEBA, p-(methacryloxyethoxy)benzaldehyde.

two vinyl groups are reacted, can be used to estimate DB; the contents of DTDMA are listed in Table 1. According to the formation mechanism of the branched copolymers proposed by Yang et al<sup>49</sup> in the controlled radical polymerization of mono- and divinyl monomers, the primary chains are formed first, and then slightly branched polymers and highly branched polymers are successively produced by coupling reactions between two primary chains and then between two slightly branched polymers. Every primary chain is terminated by a dithiobenzoate group; their number-average degree of polymerization (DP) can be estimated based on <sup>1</sup>H-NMR data. Figure 2A reveals a proton signal at  $\delta=7.52$  ppm (j), which is ascribed to the dithiobenzoate group. Based on the integral values of proton signals at  $\delta=9.86$  (a),  $\delta=2.57$  (f),  $\delta=2.5\sim 3.5$  (l), and  $\delta=7.52$  ppm (j), the DP of the primary chain was calculated, and the results are listed in Table 1. The DP of primary chains is close to their feed molar ratio (41.5), probably due to high conversion of monomers. As we know, the BPs possess a number of dithiobenzoate groups on their surface; therefore, we used the branched polymers as a macro-RAFT agent in subsequent synthesis of the BSPs.

Galactose is a specific liver-targeting ligand, which can mediate delivery of drugs to liver parenchymal cells through its strong binding with ASGP-R on the surface of the HepG2 human hepatoma cells.<sup>51,52</sup> Thus, PMAIGP was chosen as the periphery polymer of the branched star copolymers, BP(DMAEMA-co-MAEBA-co-DTDMA)(PMAIGP)<sub>n</sub>. BP-1 to BP-3 were respectively applied as a macro-RAFT agents in the RAFT polymerization of MAIGP for the synthesis of the branched star copolymers. The details of polymerization conditions and the results are listed in Table 2. The  $M_w$  and  $M_w/M_n$  values of the resultant BP(DMAEMA-co-MAEBA-co-DTDMA)(PMAIGP)<sub>n</sub> were measured by GPC, and the results are listed in Table 2. GPC traces of BSP-1, BSP-2, and BSP-3 in Figure S2 reveal that they are shifted to the high  $M_w$  region, and that the  $M_w/M_n$  values become narrower in comparison with the GPC curves of their corresponding precursors depicted in Figure S1, because RAFT polymerization

of MAIGP produced the periphery PMAIGP chains with narrow  $M_w/M_n$  values.

To estimate the compositions, and also to verify branched structure of the obtained polymers, their <sup>1</sup>H- and <sup>13</sup>C-NMR spectra were measured; a typical <sup>1</sup>H-NMR spectrum of BSP-3 is shown in Figure 2B. We can see the characteristic proton signals of MAIGP units: the anomeric proton signals appear respectively at  $\delta=3.9\sim 4.5$  (p, r, s, and t spectra peaks),  $\delta=4.62$  [n], and  $\delta=5.52$  ppm [m], and the signals at  $\delta=1.25\sim 1.60$  ppm (o) are attributed to the methyl proton of the isopropyl group. In addition, the characteristic proton signals of DMAEMA, MAEBA, and DTDMA units can be seen also; therefore, the expected BSPs have been successfully prepared. The <sup>13</sup>C-NMR spectrum of BSP-3 in Figure 3B also supports the results obtained by <sup>1</sup>H-NMR spectra; besides the characteristic carbon signals of DMAEMA, MAEBA, and DTDMA units, the characteristic carbon signals of MAIGP units appear at  $\delta=108.2$  (n), 96.1 (o), and 71.4 ppm (p); the carbon signals appearing at  $\delta=25.96$  and 24.81 ppm (q) are ascribed to the two methyl carbons of the isopropyl groups. The molar ratios of MAIGP:MAEBA:DMAEMA in BSP-1, BSP-2, and BSP-3 were calculated based on the integral ratios of the signals at  $\delta=5.50$  (m), 9.86 (a), and 2.57 ppm (f, g), and the results are listed in Table 2.

For utilization of the polymers as a drug carrier, one requisite is that the polymers should be water soluble. However, the BSPs, BSP-1 to BSP-3, are hydrophobic; thus, the MAIGP units in the periphery of the BSPs should be hydrolyzed to form water-soluble PMAGP. The hydrolysis reaction of BP(DMAEMA-MAEBA-DTDMA)(PMAIGP)<sub>n</sub> was conducted in 80% formic acid; the obtained polymer solution was dialyzed against deionized water and then lyophilized. The degree of hydrolysis was estimated by <sup>1</sup>H-NMR spectrum of the reaction product. Figure 4 is a typical <sup>1</sup>H-NMR spectrum of the BP(DMAEMA-MAEBA-DTDMA)(PMAGP)<sub>n</sub> obtained from hydrolysis of BSP-3, and we can see that the isopropylidene proton signals at  $\delta=1.2\sim 1.6$  ppm almost completely disappear, indicating that the hydrolysis reaction was successful.

**Table 2** Synthetic condition and results of BP(DMAEMA-co-MAEBA-co-DTDMA)(PMAIGP)<sub>n</sub>

No <sup>a</sup>	Macro-RAFT agent	Feed molar ratio of [MAIGP]:[RAFT agent]	Yield (%) <sup>b</sup>	$M_n$ (GPC) (g/mol) <sup>c</sup>	$M_w/M_n$ <sup>c</sup>	Molar ratio of [D]:[B]:[M] in polymer <sup>d</sup>
BSP-1	BP-1	100:1	60	20,500	1.63	10:1:24
BSP-2	BP-2	100:1	56	20,800	1.72	5:1:12
BSP-3	BP-3	100:1	64	30,600	1.69	0.8:1:2.4

**Notes:** [D], [B], [M] refer to DMAEMA, MAEBA, and MAIGP, respectively. <sup>a</sup>RAFT polymerization of MAIGP at 70°C for 24 hours respectively using BP-1, BP-2, and BP-3 as macro-RAFT agent. <sup>b</sup>Determined by gravimetry method. <sup>c</sup>Determined by GPC,  $M_n$  and  $M_w/M_n$  were calibrated based on the narrow polystyrene standards. <sup>d</sup>Molar ratios of [DMAEMA]:[MAEBA]:[MAIGP] were calculated based on <sup>1</sup>H-NMR data.

**Abbreviations:** BP(DMAEMA-co-MAEBA-co-DTDMA)(PMAIGP)<sub>n</sub>, branched poly(2-(N,N-dimethylaminoethyl)methacrylate-co-p-(methacryloyloxy)benzaldehyde-co-2,2'-dithiodiethoxyl dimethacrylate)(poly(6-O-methacryloyl-1,2; 3,4-di-O-isopropylidene-D-galactopyranose))<sub>n</sub>; BP, branched polymer; BSP, branched star polymer; No, number; RAFT, reversible addition-fragmentation chain transfer; PMAIGP, poly(6-O-methacryloylpropyl-1,2; 3,4-di-O-isopropylidene-D-galactopyranose);  $M_n$ , number-average molecular weight; GPC, gel permeation chromatography;  $M_w$ , weight-average molecular weight; <sup>1</sup>H-NMR, hydrogen-1 nuclear magnetic resonance.



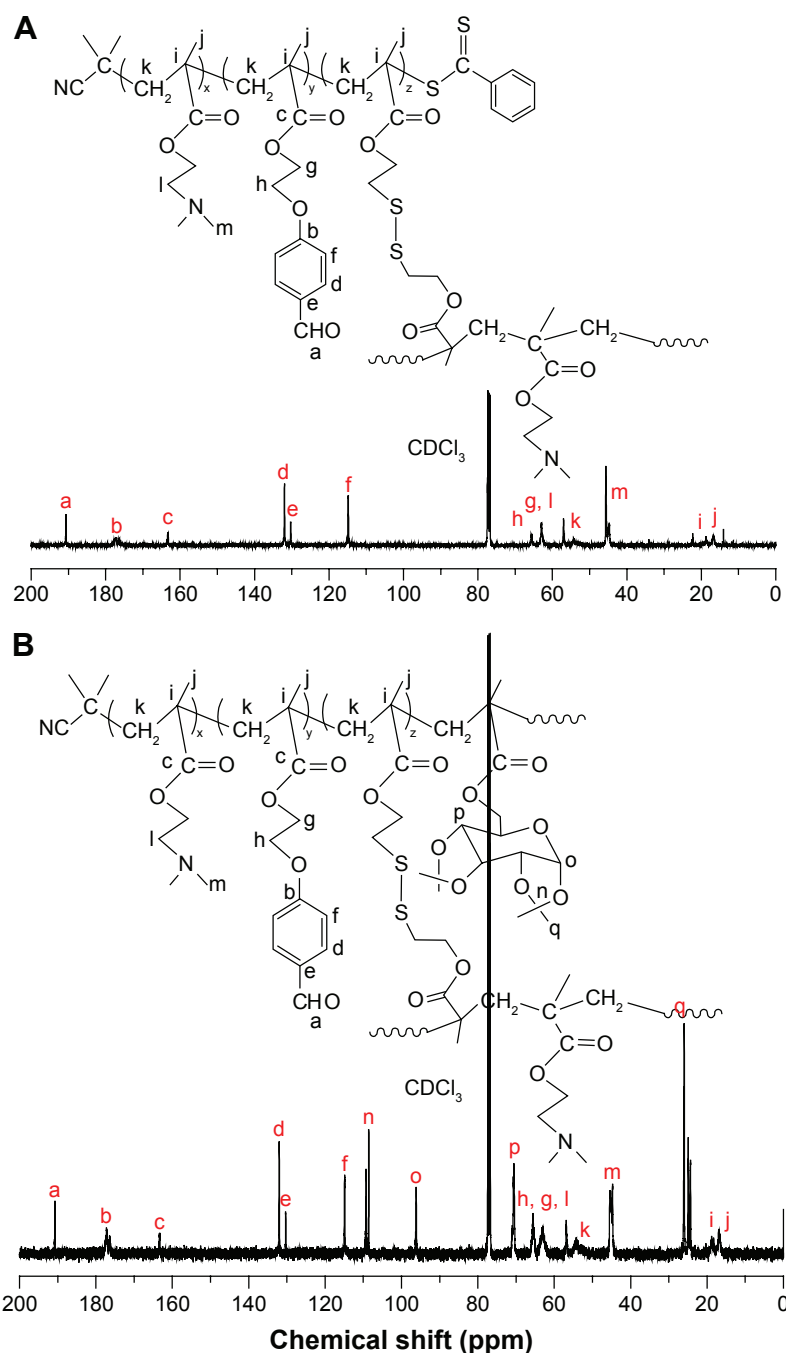


**Figure 3**  $^{13}\text{C}$ -NMR spectra of the branched polymer, BP-3 (A), and the branched star polymer, BSP-3 (B).  
**Abbreviation:**  $^{13}\text{C}$ -NMR, carbon-13 nuclear magnetic resonance.

Owing to amphiphilic properties of the hydrolyzed products, BP(DMAEMA-co-MAEBA-co-DTDMA)(PMAGP) $_n$ s, they are soluble in water to form spherical micelles, theoretically. TEM and DLS were used to characterize the assemblies, and the results are shown in Figures S3 and 5A. The TEM images in Figure S3 reveal that self-assembly of the three branched star copolymers, BSP-H1, BSP-H2, and BSP-H3, forms spherical micelles in water; their number-average diameters ( $D_{\text{TEM}}$ s) are 30–40 nm, and the size distributions are broad (Table 3). Compared to the  $D_{\text{TEM}}$ s,

the diameters obtained by DLS method are relatively big (Table 3), which is reasonable because the sizes obtained from TEM are in the dry state, whereas the size measured by DLS is in the swollen state.

### Covalent linkage of DOX onto BSP-Hs and micellization

The condensation reaction between primary amines and aldehydes is well-known in organic chemistry, and has been used in drug preparation.<sup>39,53</sup> Thus, the anti-cancer drug DOX

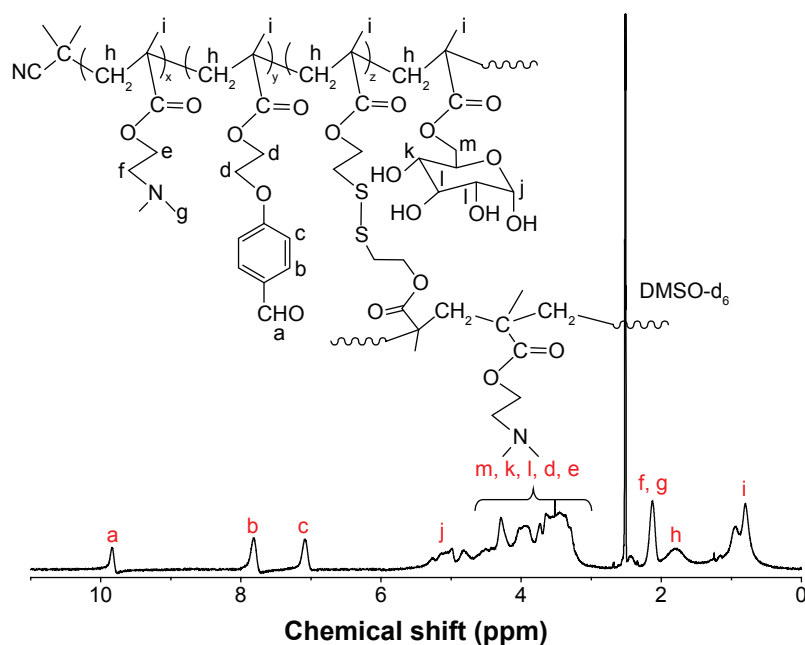


**Figure 4**  $^1\text{H-NMR}$  spectrum of the BP(DMAEMA-co-MAEBA-co-DTDMA) $_3$ (PMAGP) $_n$  in DMSO.

**Abbreviations:**  $^1\text{H-NMR}$ , hydrogen-1 nuclear magnetic resonance; BP, branched polymer; DTDMA, 2,2'-dithiodiethoxy dimethacrylate; DMAEMA, 2-(N,N-dimethylaminoethyl)methacrylate; MAEBA, p-(methacryloxyethoxy)benzaldehyde; PMAGP, poly(galactosyl methacrylate); DMSO, dimethyl sulfoxide.

was covalently linked to BSP-Hs by the reaction of primary amine in DOX with the aldehyde of MAEBA units, forming the DOX-loaded BSP-Hs via acid-labile imine linkage. To identify whether this reaction occurred, the  $^1\text{H-NMR}$  spectra of the reaction products were measured, and a typical  $^1\text{H-NMR}$  spectrum of BP(DMAEMA-co-MAEBA-co-DTDMA)(PMAGP) $_n$ -DOX is shown in Figure 5A; in addition to the characteristic proton signals of DMAEMA, MAEBA, DTDMA, and MAGP units, we can see aromatic proton signals of DOX at  $\delta = 7.20\text{--}7.72$  ppm. Therefore, the covalent linking of DOX onto the core polymer chains was successful.

Based on the weight increase of the sample and the weight of DOX added, the GEs of DOX were calculated, and the results are listed in Table 4. Since the proton signals of DOX and MAEBA overlap, the content of DOX is difficult to accurately calculate from  $^1\text{H-NMR}$  data; UV quantitative analysis was used to measure their DLCs, as well as DOX contents, based on the absorption strength alteration at 497 nm,<sup>24,54</sup> and the results are listed in Table 4. Based on the molar ratio of DMAEMA:MAEBA:DTDMA:MAGP, theoretical DLC values were calculated; they are 7.3 wt%, 13.1 wt% and 37.6 wt% for BSP-H1, BSP-H2, and BSP-H3, respectively. The measured DLCs are much lower than the corresponding theoretical values. The low GEs and DLCs are ascribed to low reaction efficiency (around 30%) of the primary amine and the aldehyde in the core of BSP-H micelles, due to the bulk of DOX.

As discussed, the hydrolyzed products of BSPs, BSP-H1, BSP-H2, and BSP-H3, are dissolved in water, forming spherical micelles. After covalently linking DOX onto the core polymer chains of the BSP-Hs, the DOX-loaded products, BSP-H-DOXs, are also dissolved in water, and the spherical micelles with BP(DMAEMA-MAEBA-DOX-DTDMA) as core and PMAGP as shell are formed, as shown in Figure 1B. To confirm the formation of core-shell micelles,  $^1\text{H-NMR}$  spectra, TEM, and DLS were used to characterize the assemblies formed. Figure 6A and B are DLS curves of the BSP-Hs and BSP-H-DOXs, respectively, and their size and size distributions are listed in Table 4. Compared to Figure 6A, the diameters of DOX-loaded BSP-Hs (90, 170, and 120 nm) are larger than that of their corresponding precursors (50, 40, and 55 nm). The reason is that covalently linking DOX onto the core polymer chains increases the hydrophobic property of the core, which is consistent with the result observed in self-assembling of asymmetric block copolymers to form crew-cut aggregates.<sup>55</sup> Figures S3 and S4 are the TEM images of BSP-Hs and BSP-H-DOXs. Comparing the micelle's size in Figure S3 with that in Figure S4, both are spherical micelles.

Since divergent agent DTDMA contains disulfide linkage the BSPs prepared from DTDMA are of redox-responsive property, such as glutathione and DTT, can degrade disulfide-containing polymers,<sup>56</sup> and these types of redox-sensitive polymers have been extensively used in drug delivery systems.<sup>57,58</sup> Thus, BP(DMAEMA-co-MAEBA-co-DTDMA)

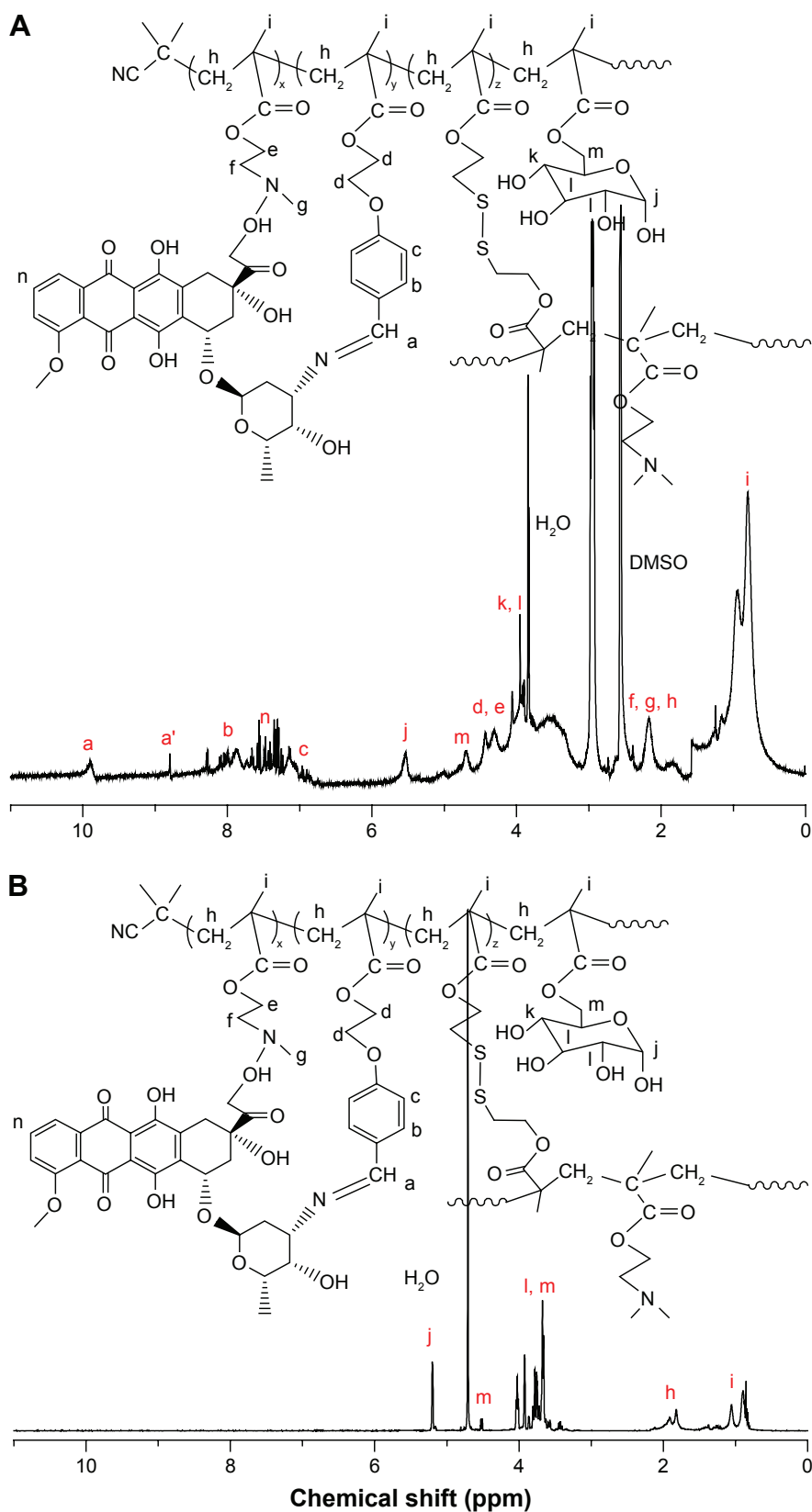


**Figure 5** <sup>1</sup>H-NMR spectra of the BP(DMAEMA-co-MAEBA-co-DTDMA)(PMAGP)<sub>n</sub>-DOX in DMSO (A), and the BP(DMAEMA-co-MAEBA-co-DTDMA)(PMAGP)<sub>n</sub>-DOX in D<sub>2</sub>O (B).

**Abbreviations:** <sup>1</sup>H-NMR, hydrogen-1 nuclear magnetic resonance; BP, branched polymer; DTDMA, 2,2'-dithiodiethyl dimethacrylate; DMAEMA, 2-(N,N-dimethylaminoethyl)methacrylate; MAEBA, p-(methacryloxyethoxy)benzaldehyde; PMAGP, poly(6-O-methacryloyl-D-galactopyranose); DOX, doxorubicin; DMSO, dimethyl sulfoxide; D<sub>2</sub>O, deuterium oxide.

**Table 3** Characteristics of the BP(DMAEMA-co-MAEBA-co-DTDMA)(PMAGP)<sub>n</sub> micelles

No <sup>a</sup>	Precursor	D <sub>DLS</sub> (nm) <sup>b</sup>	PDI <sup>b</sup>	D <sub>TEM</sub> (nm) <sup>c</sup>
BSP-H1	BSP-1	50	0.282	40
BSP-H2	BSP-2	40	0.361	30
BSP-H3	BSP-3	55	0.142	50

**Notes:** <sup>a</sup>Hydrolysis of BSP-1, BSP-2, and BSP-3 in 80% formic acid solution at room temperature for 3 days. <sup>b</sup>D<sub>DLS</sub> and PDI are average diameter and size distribution, respectively, of the BP(DMAEMA-co-MAEBA-co-DTDMA)(PMAGP)<sub>n</sub> micelles, which were measured by dynamic light (DLS) scattering method. <sup>c</sup>D<sub>TEM</sub>s are average diameters measured by transmission electron microscopy (TEM) method.

**Abbreviations:** BP(DMAEMA-co-MAEBA-co-DTDMA)(PMAIGP)<sub>n</sub>, branched poly(2-(N,N-dimethylaminoethyl)methacrylate-co-p-(methacryloylethoxy)benzaldehyde-co-2,2'-dithiodiethoxyl dimethacrylate)(poly(6-O-methacryloyl-1,2; 3,4-di-O-isopropylidene-D-galactopyranose)); BSP, branched star polymer; No, number; PMAGP, poly(6-O-methacryloyl-D-galactopyranose); PDI, polydispersity.

(PMAGP)<sub>n</sub> was treated with 10 mM DTT in deionized water at room temperature for 48 hours; then, the degraded products were analyzed by GPC. For comparison, GPC traces of both BSP-H3 and its degraded products are shown in Figure 7, and the  $M_w$  of the products obtained after treatment with DTT is significantly decreased from 30,600 g/mol to 7,600 g/mol, due to cleavage of the disulfide linkage in the branching units.

## In vitro DOX release

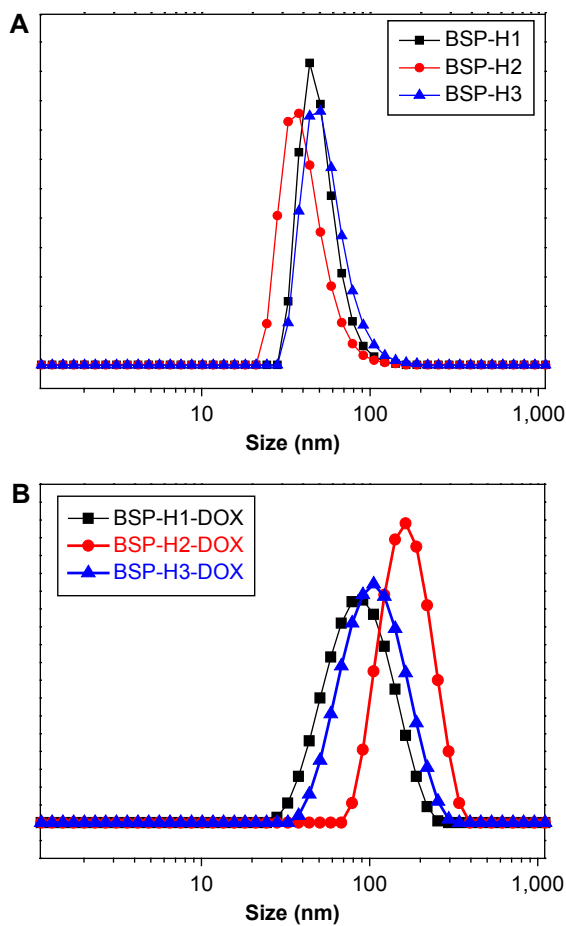
Efficient release of DOX from BSP-H-DOX micelles is crucial for drug delivery systems. Thus, we tested drug release behavior of the BSP-H3-DOX micelles in the PBS solutions at pH 5.0, 6.0, and 7.4, with or without DTT (10 mM), and the results are shown in Figure 8. As described, the imine linkage is acid-labile, and the aromatic imine bond is stable at the physiological pH. When the release was conducted in an aqueous solution at pH = 7.4 with or without DTT, almost no DOX in the drug-loaded micelles was released, which is consistent with the hydrolysis results of isatin-based aryl imine derivatives.<sup>37</sup>

**Table 4** Characterizations of BP(DMAEMA-co-MAEBA-co-DTMA)(PMAGP)<sub>n</sub>-DOX micelles

Sample	D <sub>DLS</sub> (nm) <sup>a</sup>	PDI <sup>b</sup>	DLC <sub>NMR</sub> (wt%) <sup>c</sup>	DLC <sub>UV</sub> (wt%) <sup>d</sup>	GE (wt%) <sup>e</sup>
BSP-H1-DOX	90	0.221	4.67	2.1	4.46
BSP-H2-DOX	170	0.109	6.24	4.3	5.87
BSP-H3-DOX	120	0.153	15.9	12.7	13.7

**Notes:** <sup>a</sup>D<sub>DLS</sub> refers to average diameters (D) of the BP(DMAEMA-co-MAEBA-co-DTDMA)(PMAGP)<sub>n</sub> micelles, which were measured by DLS method. <sup>b</sup>PDI refers to size distribution of the micelles as measured by dynamic light scattering (DLS) method; <sup>c</sup>DLC refers to drug-loaded content, which was estimated based on <sup>1</sup>H-NMR data. <sup>d</sup>Determined by ultraviolet (UV) quantitative analysis. <sup>e</sup>Determined by gravimetric method.

**Abbreviations:** BP(DMAEMA-co-MAEBA-co-DTDMA)(PMAIGP)<sub>n</sub>, branched poly(2-(N,N-dimethylaminoethyl)methacrylate-co-p-(methacryloylethoxy)benzaldehyde-co-2,2'-dithiodiethoxyl dimethacrylate)(poly(6-O-methacryloyl-1,2; 3,4-di-O-isopropylidene-D-galactopyranose)); GE, grafting efficiency; BSP, branched star polymer; NMR, nuclear magnetic resonance; <sup>1</sup>H-NMR, hydrogen-1 nuclear magnetic resonance; DOX, doxorubicin; PMAGP, poly(6-O-methacryloyl-D-galactopyranose); PDI, polydispersity; BSP-H-DOX, DOX-loaded product.

**Figure 6** DLS curves of the micelles prepared from BSP-H1, BSP-H2, and BSP-H3 (A), and BSP-H-DOX pro-drug variants (B).

**Abbreviations:** DLS, dynamic light scattering; BSP, branched star polymer; DOX, doxorubicin.

Obvious contribution of the reducing agent DTT to the drug release was not observed, because DOX is covalently bonded to the polymer chains via aromatic imine linkage, which is stable in the neutral aqueous solution.<sup>36-39</sup> However, when the release was performed in weak acidic solution, the influence of DTT on the release of DOX was observed; for example, when the release was conducted at pH = 6.0 with and without DTT for 48 hours, different release rates were observed: 44 wt% (with DTT) and 34 wt% (without DTT) of DOX in micelles were released. The same phenomenon was observed for the release at pH = 5.0, 56 wt% (with DTT) and 47 wt% (without DTT) of DOX in the drug carrier were released after 48 hours, because more imine bonds of the MAEBA units were exposed to an acidic environment after degradation of the BSP-H chains, which in turn, accelerated disassembly of the micelles. Acidity of the solution was another important factor influencing release of the drug. When pH values of the solution decreased from 6.0 to 5.0 with and without DTT, the release rates of DOX from the micelles increased,

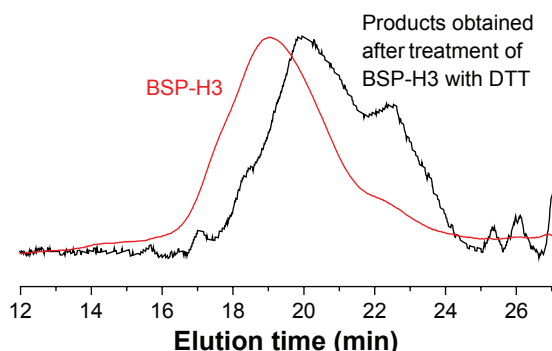


**Figure 7** GPC curves of the BP(DMAEMA-co-MAEBA-co-DTDMA)(PMAGP)<sub>n</sub> with  $M_n = 30,600$  g/mol (BSP-H3), and the degraded products ( $M_n = 7,600$  g/mol) after BSP-H3 was treated with DTT at room temperature for 48 hours.

**Abbreviations:** GPC, gel permeation chromatography; BP, branched polymer; BSP, branched star polymer; DTDMA, 2,2'-dithiodiethoxy dimethacrylate; DMAEMA, 2-(N,N-dimethylaminoethyl)methacrylate; MAEBA, p-(methacryloxyethoxy)benzaldehyde; PMAGP, poly(6-O-methacryloyl-D-galactopyranose); DTT, dithiothreitol; min, minutes.

and the amount of DOX released from the drug carriers was enhanced, also shown in Figure 8.

## In vitro cytotoxicity assay

Cytotoxicity of BSP-H and BSP-H-DOX micelles was evaluated by MTT assay, and HepG2 and HeLa cells were used in the current study. The cells were incubated with various concentrations of the BSP-H3 micellar solutions at 37°C for 24 hours, and the cells treated without the micelles were used as a control. The results in Figure 9 show virtually no toxicity of BP(DMAEMA-co-MAEBA-co-DTDMA)(PMAGP)<sub>n</sub> micelles without DOX in the entire concentration range tested to both HepG2 and HeLa cells; thus, BSP-H3s are of very low cytotoxicity.

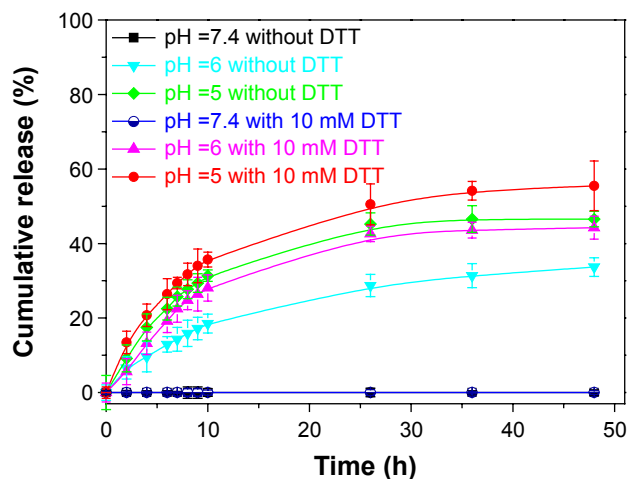


**Figure 8** DOX release profiles of the branched star polymer-DOX, BSP-H3-DOX micelles in the aqueous buffer solution under different conditions: at pH =7.4 with and without 10 mM DTT; at pH =6.0 with and without 10 mM DTT; and at pH =5.0 with and without 10 mM DTT.

**Note:** The dark blue line hides the appearance of the black line in the figure.

**Abbreviations:** DOX, doxorubicin; DTT, dithiothreitol; h, hours.

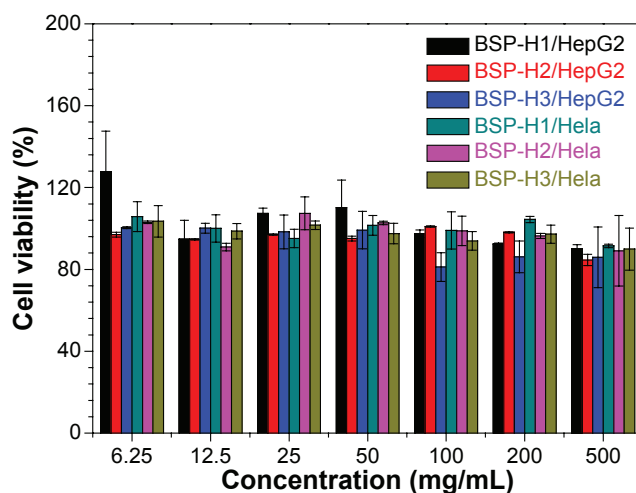


**Figure 9** Relative cell viability of HeLa and HepG2 cells evaluated by MTT assay after incubation with micellar solution of the branched star polymers (BSP-H1, BSP-H2, and BSP-H3) at pH =7.4.

**Abbreviation:** MTT, 3-(4,5-dimethylthiazol-2-yl)-2,5-diphenyltetrazolium bromide.

The cytotoxicity results of free DOX and BSP-H3-DOX are shown in Figure 10. The HepG2 and HeLa cells in solutions of free DOX displayed different dose-response curves, and DOX exhibited higher cytotoxicity to HepG2 cells than to the HeLa cells; for example, DOX doses required for 50% cellular growth inhibition ( $IC_{50}$ ), evaluated in HepG2 cells and HeLa cells, were  $\sim 0.47$   $\mu\text{g/mL}$  and  $\sim 1.64$   $\mu\text{g/mL}$ , respectively. In testing cytotoxicity of the pro-drug, BSP-H3-DOX, to HepG2 and HeLa cells, two different dose-response curves with  $IC_{50}$  values of 50  $\mu\text{g/mL}$  and 6.62  $\mu\text{g/mL}$ , respectively, were observed. Since BSP-Hs do not display cytotoxicity (Figure 9), it is reasonable to posit that cytotoxicity of the

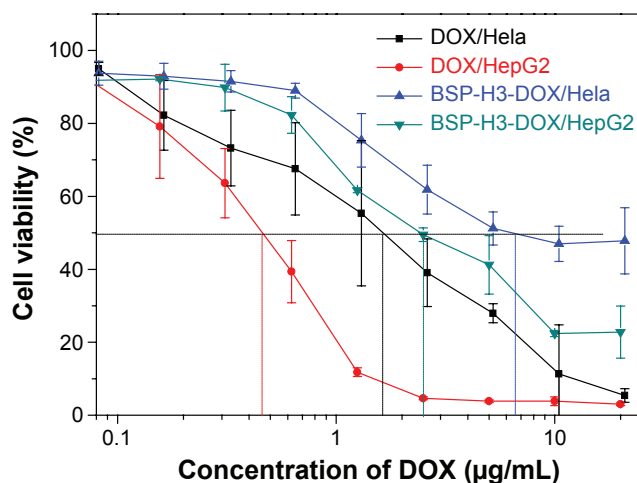


**Figure 10** Relative cell viability of HeLa and HepG2 cells evaluated by MTT assay after incubation with solution of the BSP-H3-DOX micelles at pH =7.4 and free DOX at pH =7.4. Incubating temperature, 37°C; time, 24 hours.

**Abbreviations:** MTT, 3-(4,5-dimethylthiazol-2-yl)-2,5-diphenyltetrazolium bromide; BSP, branched star polymer; DOX, doxorubicin.

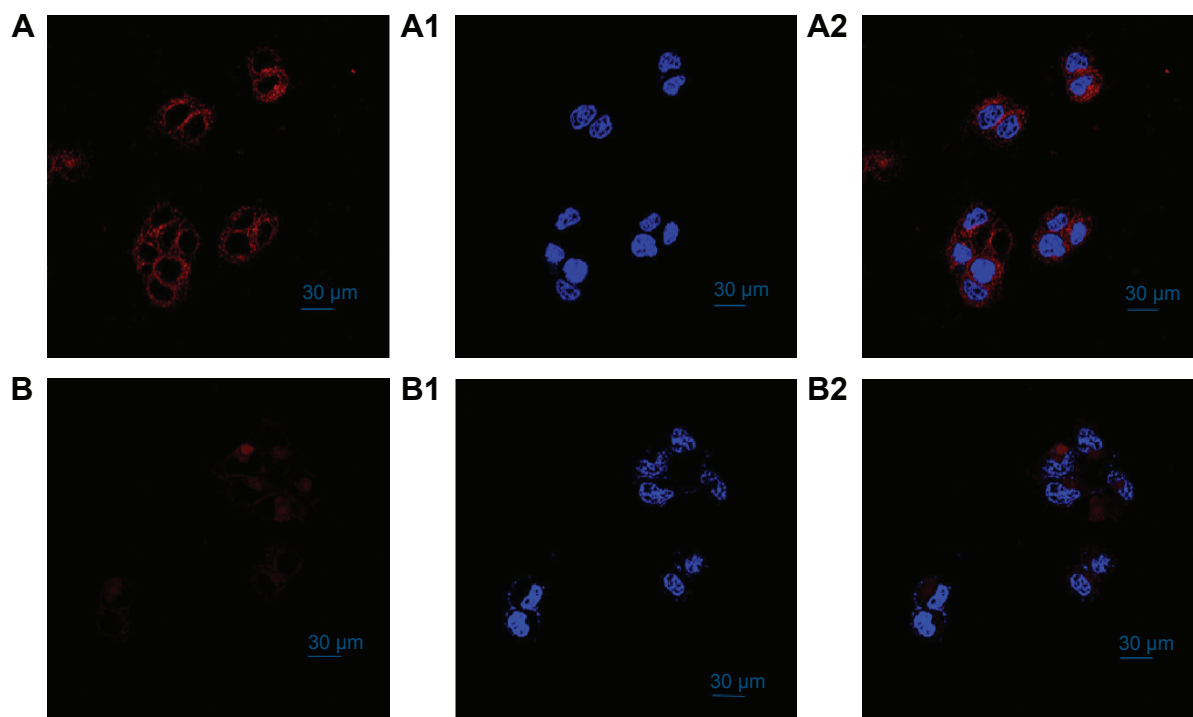


**Figure 11** Confocal laser scanning microscope images of the HepG2 cells (**A**) and the HeLa cells (**B**) treated with the BSP-H3-DOX micelle solution (**A1** and **B1**) and stained with DAPI (**A2** and **B2**) at 37°C for 4 hours for each panel; the images, from left to right, show DOX (red), DAPI (blue), and a merge of the two images (far right, red and blue).

**Abbreviations:** BSP, branched star polymer; DOX, doxorubicin; DAPI, 2-(4-amidinophenyl)-6-indolecarbamidine dihydrochloride.

pro-drug comes from release of DOX in the micelles. In addition, HSP-H3-DOX micelles showed higher cytotoxicity to HepG2 cells compared to HeLa cells.

## Cellular uptake

The cellular uptake efficiency of HSP-H-DOX micelles was further studied by CLSM. HepG2 cells and HeLa cells were incubated with the same dose of the HSP-H3-DOX micelles for 4 hours, and then were stained with DAPI. CLSM images in Figure 11 reveal that DOX red fluorescence appears at the perinuclear region of HepG2 cells, and that DAPI blue fluorescence is located at the nucleus, suggesting successful internalization of the micelles within the cells. Moreover, DOX red fluorescence in HeLa cells (Figure 11B1) is relatively weak in comparison with that in HepG2 cells (Figure 11A1). As discussed, galactose is a specific liver-targeting ligand;<sup>51,52</sup> the periphery polymers, PMAGPs, contain a number of galactose groups, and therefore, HSP-H-DOXs can be easily internalized by HepG2 cells compared to HeLa cells.

## Conclusion

In the current study, amphiphilic branched star copolymers, BP(DMAEMA-co-MAEBA-co-DTDMA)(PMAGP)<sub>n</sub>s,

which possess pH- and redox-responsive properties, have been successfully synthesized by RAFT polymerization, and the anti-cancer drug, DOX, has been linked to the branched copolymers, BP(DMAEMA-co-MAEBA-co-DTDMA)s, by condensation reaction of primary amine of DOX with aldehyde groups of the polymer chains. The resultant DOX-containing BSP-Hs can be self-assembled in water, forming DOX-loaded spherical micelles. Aromatic imine linkage is quite stable in neutral water, but is pH-sensitive, and controlled release of DOX from BSP-H-DOX micelles is achieved under weak acidic condition (pH =5 and 6). Degradation of branched star copolymers under DTT can accelerate release of the drug in micelles. Experimental results in vitro reveal almost no cytotoxicity of BP(DMAEMA-co-MAEBA-co-DTDMA)(PMAGP)<sub>n</sub>s in the current study, and the release of DOX in HepG2 and HeLa cells was observed. DOX-loaded micelles displayed specific binding to HepG2 cells, due to galactosyl groups on the periphery of micelles. Thus, this kind of polymer micelle can act as a hepatoma-targeting drug delivery vehicle.

## Acknowledgments

This work was supported by National Natural Science Foundation of China under contract numbers 21090354

and 21374107, and was also supported by the Fundamental Research Funds for the Central Universities (grant number WK 2060200012).

## Disclosure

The authors report no conflicts of interest in this work.

## References

- Phillips MA, Gran ML, Peppas NA. Targeted nanodelivery of drugs and diagnostics. *Nano Today*. 2010;5:143–159.
- Liu S, Maheshwari R, Kiick KL. Polymer-based therapeutics. *Macromolecules*. 2009;42:3–13.
- Peer D, Karp JM, Hong S, Farokhzad OC, Margalit R, Langer R. Nanocarriers as an emerging platform for cancer therapy. *Nat Nanotechnol*. 2007;2:751–760.
- Kim BS, Park SW, Hammond PT. Hydrogen-bonding layer-by-layer-assembled biodegradable polymeric micelles as drug delivery vehicles from surfaces. *ACS Nano*. 2008;2:386–392.
- Torchilin VP. Multifunctional nanocarriers. *Adv Drug Deliv Rev*. 2006;58:1532–1555.
- Kataoka K, Harada A, Nagasaki Y. Block copolymer micelles for drug delivery: design, characterization and biological significance. *Adv Drug Deliv Rev*. 2001;47:113–131.
- Su W, Luo XH, Wang HF, et al. Hyperbranched polycarbonate-based multimolecular micelle with enhanced stability and loading efficiency. *Macromol Rapid Commun*. 2011;32:390–396.
- Zhou Y, Yan D. Supramolecular self-assembly of amphiphilic hyperbranched polymers at all scales and dimensions: progress, characteristics and perspectives. *Chem Commun (Camb)*. 2009;10:1172–1188.
- Meng F, Zhong Z, Feijen J. Stimuli-responsive polymersomes for programmed drug delivery. *Biomacromolecules*. 2009;10:197–209.
- Guo X, Shi C, Wang J, Di S, Zhou S. pH-triggered intracellular release from actively targeting polymer micelles. *Biomaterials*. 2013;34:4544–4554.
- Shi C, Guo X, Qu Q, Tang Z, Wang Y, Zhou S. Actively targeted delivery of anticancer drug to tumor cells by redox-responsive star-shaped micelles. *Biomaterials*. 2014;35:8711–8722.
- Duncan R. The dawning era of polymer therapeutics. *Nat Rev Drug Discov*. 2003;2:347–360.
- Wang Y, Hong CY, Pan CY. Spiropyran-based hyperbranched star copolymer: synthesis, phototropy, FRET, and bioapplication. *Biomacromolecules*. 2012;13:2585–2893.
- Lee CC, MacKay JA, Fréchet JM, Szoka FC. Designing dendrimers for biological applications. *Nature Biotechnol*. 2005;23:1517–1526.
- Medina SH, El-Sayed ME. Dendrimers as carriers for delivery of chemotherapeutic agents. *Chem Rev*. 2009;109:3141–3157.
- Fox ME, Szoka FC, Fréchet JM. Soluble polymer carriers for the treatment of cancer: the importance of molecular architecture. *Acc Chem Res*. 2009;42:1141–1151.
- Liu J, Pang Y, Huang W, et al. Bioreducible micelles self-assembled from amphiphilic hyperbranched multiarm copolymer for glutathione-mediated intracellular drug delivery. *Biomacromolecules*. 2011;12:1567–1577.
- Shi F, Ding J, Xiao C, et al. Intracellular microenvironment responsive PEGylated polypeptide nanogels with ionizable cores for efficient doxorubicin loading and triggered release. *J Mater Chem*. 2012;22:14168–14179.
- Kong SD, Sartor M, Hu CM, Zhang W, Zhang L, Jin S. Magnetic field activated lipid-polymer hybrid nanoparticles for stimuli-responsive drug release. *Acta Biomater*. 2013;9:5447–5452.
- Dai M, Xu X, Song J, et al. Preparation of camptothecin-loaded PCEC microspheres for the treatment of colorectal peritoneal carcinomatosis and tumor growth in mice. *Cancer Lett*. 2011;312:189–196.
- Johnson JA, Lu YY, Burtis AO, et al. Drug-loaded, bivalent-bottle-brush polymers by graft-through ROMP. *Macromolecules*. 2010;43:10326–10335.
- Cheetham AG, Zhang P, Lin YA, Lock LL, Cui H. Supramolecular nanostructures formed by anticancer drug assembly. *J Am Chem Soc*. 2013;135:2907–2910.
- Cho JK, Chun C, Kuh HJ, Song SC. Injectable poly(organophosphazene)-camptothecin conjugate hydrogels: synthesis, characterization, and antitumor activities. *Eur J Pharm Biopharm*. 2012;81:582–590.
- Wang Y, Hong CY, Pan CY. Galactose-based amphiphilic block copolymers: synthesis, micellization, and bioapplication. *Biomacromolecules*. 2013;14:1444–1451.
- Ding J, Xu W, Zhang Y, et al. Self-reinforced endocytoses of smart polypeptide nanogels for “on-demand” drug delivery. *J Control Release*. 2013;172:444–455.
- Lynn DM, Amiji MM, Langer R. pH-responsive polymer microspheres: rapid release of encapsulated material within the range of intracellular pH. *Angew Chem Int Ed Engl*. 2001;40:1707–1710.
- Lee S, Saito K, Lee HR, et al. Hyperbranched double hydrophilic block copolymer micelles of poly(ethylene oxide) and polyglycerol for pH-responsive drug delivery. *Biomacromolecules*. 2012;13:1190–1196.
- Zhan F, Chen W, Wang Z, et al. Acid-activatable prodrug nanogels for efficient intracellular doxorubicin release. *Biomacromolecules*. 2011;12:3612–3620.
- Bae Y, Jang WD, Nishiyama N, Fukushima S, Kataoka K. Multifunctional polymeric micelles with folate-mediated cancer cell targeting and pH-triggered drug releasing properties for active intracellular drug delivery. *Mol Biosyst*. 2005;1:242–250.
- Tang X, Pan CY. Double hydrophilic block copolymers PEO-b-PGA: synthesis, application as potential drug carrier and drug release via pH-sensitive linkage. *J Biomed Mater Res A*. 2008;86:428–438.
- Gillies ER, Fréchet JM. pH-responsive copolymer assemblies for controlled release of doxorubicin. *Bioconjug Chem*. 2005;16:361–368.
- Jaeger DA, Sayed YM. Synthesis and characterization of single-chain second generation cleavable surfactants. *J Org Chem*. 1993;58:2619–2627.
- Xu S, Luo Y, Haag R. Water-soluble pH-responsive dendritic core-shell nanocarriers for polar dyes based on poly(ethylene imine). *Macromol Biosci*. 2007;7:968–974.
- Lemieux GA, Bertozzi CR. Chemoselective ligation reactions with proteins, oligosaccharides and cells. *Trends Biotechnol*. 1998;16:506–513.
- Kaneko T, Willner D, Monková I, et al. New hydrazone derivatives of adriamycin and their immunoconjugates – a correlation between acid stability and cytotoxicity. *Bioconjug Chem*. 1991;2:133–141.
- Ding C, Gu J, Qu X, Yang Z. Preparation of multifunctional drug carrier for tumor-specific uptake and enhanced intracellular delivery through the conjugation of weak acid labile linker. *Bioconjug Chem*. 2009;20:1163–1170.
- Matesic L, Locke JM, Vine KL, Ranson M, Bremner JB, Skropeta D. Synthesis and hydrolytic evaluation of acid-labile imine-linked cytotoxic itatin model systems. *Bioorg Med Chem*. 2011;19:1771–1778.
- Müller IA, Kratz F, Jung M, Warnecke A. Schiff bases derived from p-aminobenzyl alcohol as trigger groups for pH-dependent prodrug activation. *Tetrahedron Lett*. 2010;51:4371–4374.
- Sedlák M, Pravda M, Staud F, Kubíčová L, Týcová K, Ventura K. Synthesis of pH-sensitive amphotericin B-poly(ethylene glycol) conjugates and study of their controlled release in vitro. *Bioorg Med Chem*. 2007;15:4069–4076.
- Xu X, Flores JD, McCormick CL. Reversible imine shell cross-linked micelles from aqueous RAFT-synthesized thermoresponsive triblock copolymers as potential nanocarriers for “pH-triggered” drug release. *Macromolecules*. 2011;44:1327–1334.
- Kim YH, Park JH, Lee M, Kim YH, Park TG, Kim SW. Polyethyleneimine with acid-labile linkages as a biodegradable gene carrier. *J Control Release*. 2005;103:209–219.
- Jackson AW, Fulton DA. pH triggered self-assembly of core cross-linked star polymers possessing thermoresponsive cores. *Chem Commun (Camb)*. 2011;47:6807–6809.

43. Jackson AW, Stakes C, Fulton DA. The formation of core cross-linked star polymer and nanogel assemblies facilitated by the formation of dynamic covalent imine bonds. *Polym Chem*. 2011;2:2500–2511.
44. Murray BS, Jackson AW, Mahon CS, Fulton DA. Reactive thermo-responsive copolymer scaffolds. *Chem Commun (Camb)*. 2010;46:8651–8653.
45. Hu X, Li H, Luo S, Liu T, Jiang Y, Liu S. Thiol and pH dual-responsive dynamic covalent shell cross-linked micelles for triggered release of chemotherapeutic drugs. *Polym Chem*. 2013;4:695–706.
46. Hu X, Tian J, Liu T, Zhang G, Liu S. Photo-triggered release of caged camptothecin prodrugs from dually responsive shell cross-linked micelles. *Macromolecules*. 2013;46:6243–6256.
47. Hong CY, You YZ, Liu J, Pan CY. Dendrimer-star polymer and block copolymer prepared by reversible addition-fragmentation chain transfer (RAFT) polymerization with dendritic chain transfer agent. *J Polym Sci Part A: Polym Chem*. 2005;43:6379–6393.
48. Zheng Q, Pan CY. Synthesis and characterization of dendrimer–star polymer using dithiobenzoate-terminated poly(propylene imine) dendrimer via reversible addition–fragmentation transfer polymerization. *Macromolecules*. 2005;38:6841–6848.
49. Yang HJ, Jiang BB, Huang WY, et al. Development of branching in atom transfer radical copolymerization of styrene with triethylene glycol dimethacrylate. *Macromolecules*. 2009;42:5976–5982.
50. Sun M, Pan CY. Formation of hyperbranched polymers in atom transfer radical copolymerization of MMA and DVB. *Sci China Chem*. 2010;53:2440–2451.
51. Mamidyala SK, Dutta S, Chrunyk BA, et al. Glycomimetic ligands for the human asialoglycoprotein receptor. *J Am Chem Soc*. 2012;134:1978–1981.
52. Mi FL, Wu YY, Chiu YL, et al. Synthesis of a novel glycoconjugated chitosan and preparation of its derived nanoparticles for targeting HepG2 cells. *Biomacromolecules*. 2007;8:892–898.
53. Sedláč M, Pravda M, Kubicová L, Mikulčíková P, Ventura K. Synthesis and characterisation of a new pH-sensitive amphotericin B–poly(ethylene glycol)-*b*-poly(L-lysine) conjugate. *Bioorg Med Chem Lett*. 2007;17:2554–2557.
54. Cartoni A, Menna P, Salvatorelli E, et al. Oxidative degradation of cardiotoxic anticancer anthracyclines to phthalic acids. Novel function or ferrylmyoglobin. *J Biol Chem*. 2004;279:5088–5099.
55. Zhang L, Eisenberg A. Formation of crew-cut aggregates of various morphologies from amphiphilic block copolymers in solution. *Polym Adv Technol*. 1998;9:677–699.
56. Balendiran GK, Dabur R, Fraser D. The role of glutathione in cancer. *Cell Biochem Funct*. 2004;22:343–352.
57. Xie LL, Xu JQ, Gao CY. Multilayers and poly(allylamine hydrochloride)-graft-poly(ethylene glycol) modified bovine serum albumin nanoparticles: improved stability and pH-responsive drug delivery. *Chinese J Polym Sci*. 2012;30:719–726.
58. Yang W, Pan CY, Liu XQ, Wang J. Multiple functional hyperbranched poly(amido amine) nanoparticles: synthesis and application in cell imaging. *Biomacromolecules*. 2011;12:1523–1531.



## Supplementary materials

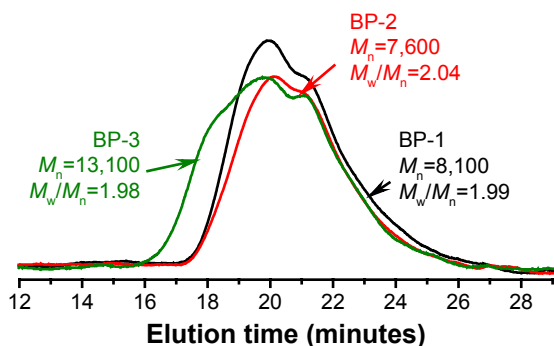


**Figure S1** GPC curves of the branched polymers, BP(DMAEMA-MAEBA-DTDMA)-1 (BP-1), BP(DMAEMA-MAEBA-DTDMA)-2 (BP-2), and BP(DMAEMA-MAEBA-DTDMA)-3 (BP-3) prepared by RAFT copolymerization at 70°C for 24 hours with feed molar ratios of [DMAEMA]:[MAEBA]:[DTDMA]:[CPDA]:[AIBN] = 36:4:1.5:1:0.25, 32:8:1.5:1:0.25, and 16:24:1.5:1:0.25, respectively.

**Abbreviations:** GPC, gel permeation chromatography; BP, branched polymer; DTDMA, 2,2'-dithiodiethoxy dimethacrylate; DMAEMA, 2-(N,N-dimethylaminoethyl)methacrylate; MAEBA, p-(methacryloxyethoxy)benzaldehyde; RAFT, reversible addition-fragmentation chain transfer; CPDB, cyanoisopropyl dithiobenzoate; AIBN, Azobis(isobutyronitrile).

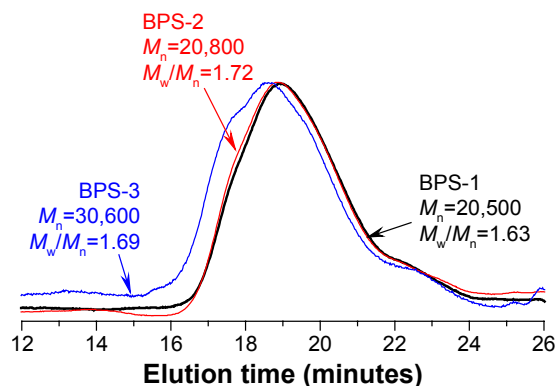


**Figure S2** GPC curves of the branched star polymers (BSPs), BP(DMAEMA-MAEBA-DTDMA)1(PMAIGP)<sub>n</sub> (BSP-1), BP(DMAEMA-MAEBA-DTDMA)2(PMAIGP)<sub>n</sub> (BSP-2), and BP(DMAEMA-MAEBA-DTDMA)3(PMAIGP)<sub>n</sub> (BSP-3) prepared by RAFT polymerization of MAIGP at 70°C for 24 hours with the feed molar ratios of [MAIGP]:[BP-1 or BP-2 or BP-3] = 100:1.

**Abbreviations:** GPC, gel permeation chromatography; BP, branched polymer; DTDMA, 2,2'-dithiodiethoxy dimethacrylate; DMAEMA, 2-(N,N-dimethylaminoethyl)methacrylate; MAEBA, p-(methacryloxyethoxy)benzaldehyde; RAFT, reversible addition-fragmentation chain transfer; CPDB, cyanoisopropyl dithiobenzoate; AIBN, Azobis(isobutyronitrile); MAIGP, poly(6-O-methacryloyl-1,2; 3,4-di-O-isopropylidene-D-galactopyranose).

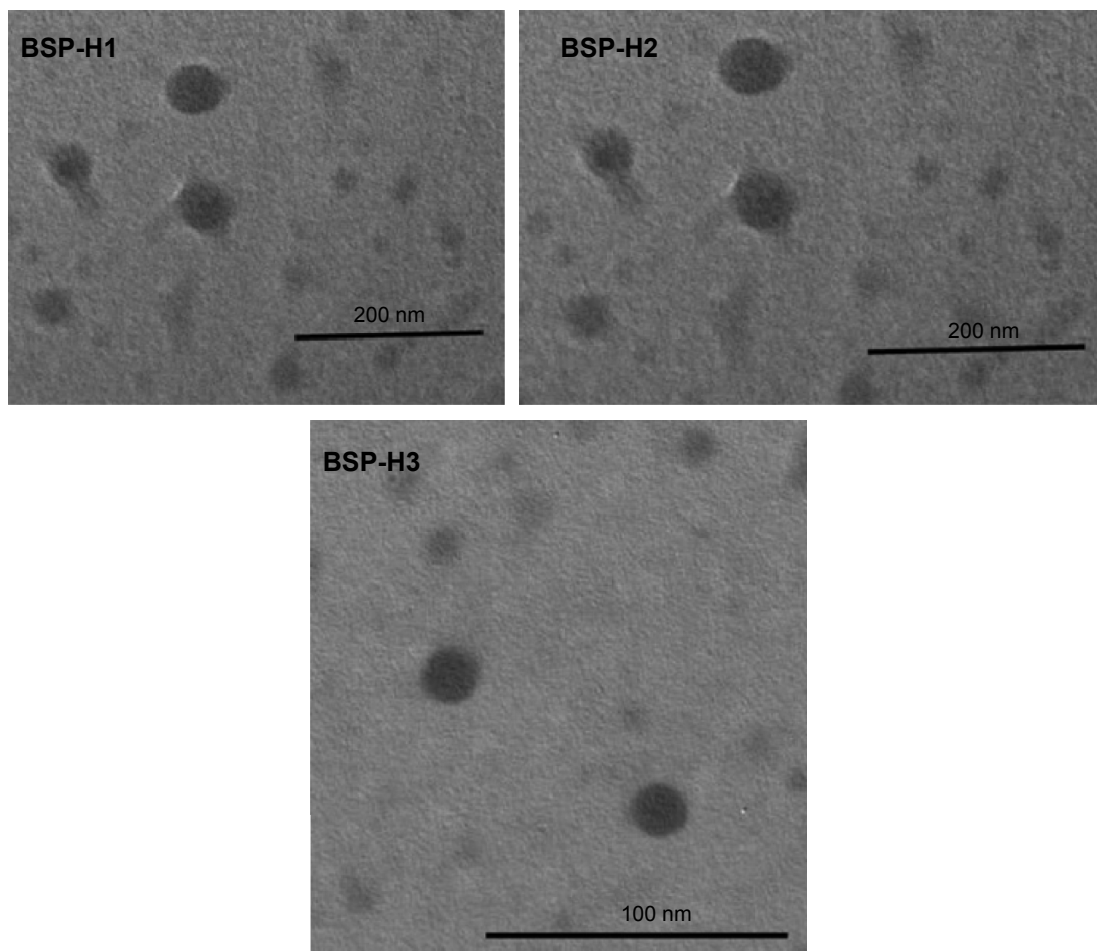


**Figure S3** TEM images of the micelles prepared respectively from BSP-H1 to BSP-H3.

**Abbreviations:** TEM, transmission electron microscopy; BSP, branched star polymer.

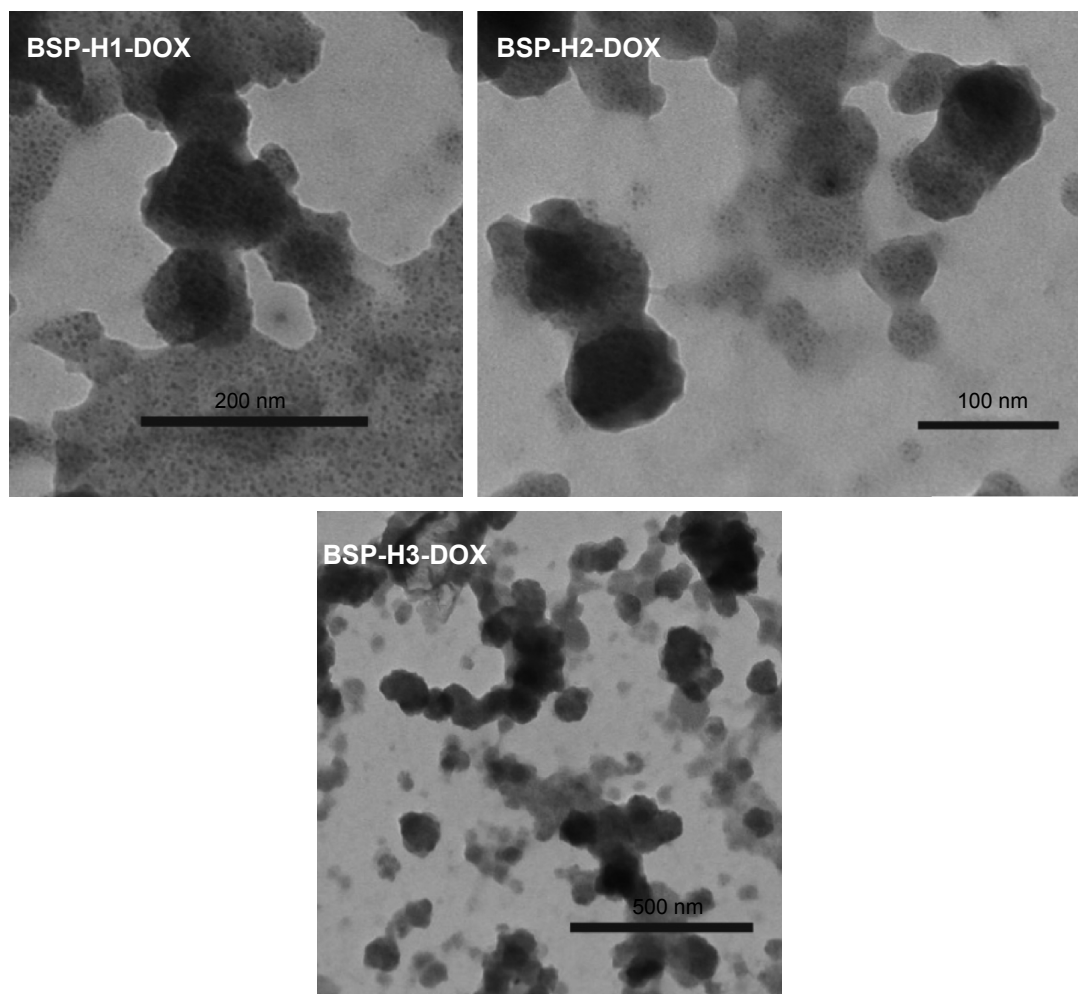


**Figure S4** TEM images of BSP-H-DOX pro-drug.

**Abbreviations:** TEM, transmission electron microscopy; BSP, branched star polymer; DOX, doxorubicin.

### International Journal of Nanomedicine

## Publish your work in this journal

The International Journal of Nanomedicine is an international, peer-reviewed journal focusing on the application of nanotechnology in diagnostics, therapeutics, and drug delivery systems throughout the biomedical field. This journal is indexed on PubMed Central, MedLine, CAS, SciSearch®, Current Contents®/Clinical Medicine,

Submit your manuscript here: <http://www.dovepress.com/international-journal-of-nanomedicine-journal>

Dovepress

Journal Citation Reports/Science Edition, EMBase, Scopus and the Elsevier Bibliographic databases. The manuscript management system is completely online and includes a very quick and fair peer-review system, which is all easy to use. Visit <http://www.dovepress.com/testimonials.php> to read real quotes from published authors.